On the Origin and the Properties of the Blue Emission in an NaCl:Cu^+ Crystal

Toshio KUROBORI* and Hayato YONEZAWA**

Abstract

The origin and the properties of a recently found blue emission at 420 nm in an NaCl :Cu^+:OH^- crystal are investigated. In order to obtain further evidence, various experiments such as the isotopic substitution, the luminescence decay curves and the temperature dependence of its emission, are systematically performed. A drastic wavelength shift of its peak position by 27 nm has been observed at the temperature of ~170 K. As a result the origin of its emission is qualitatively discussed and the activation energy corresponding to its transition is also estimated.

Introduction

It is known that the optical and electrical properties of the alkali halide are affected by impurities. Among the many impurities the hydroxyl ion (OH^-) is one of the common impurities in the alkali halides and is easily incorporated in these crystals without the intentional addition of impurities during various thermal treatments as well as preparation for crystal growth. It is also known that the presence of OH^- ions in these crystals leads to some drastic effects such as the depression of the ionic conductivity due to the formation Mg^{2+}-OH^- complexes in LiF[1], the increase of the dielectric constant of KCl by OH^- doping[2] and the enhancement of F-center formation after exposure to ionizing radiation in the OH^--doped NaCl or KCl samples[3]. In addition to these effects, decomposition of OH^- at low temperatures yields H^-, H^0, O^- and O_2^- ions upon U.V. or X-irradiation[4]. Such a photochemical process following irradiation of OH^- doped alkali halides has been playing an important role in the field of color center lasers. It has been demonstrated[5,6] that the OH^- impurity is one of the most useful candidates for stabilizing the pure F_2^+-center, consisting of two adjacent halogen vacancies along the ⟨110⟩ direction of the crystal with a single trapped electron. As a result the stable $(F_2^+)^{**}$[7], $(F_2^+)_H$[8-11] and $(F_2^+)_{AH}$ centers[12] have been successfully developed in various host crystals by doping the starting material

平成5年9月6日受理

* *Dep. of Materials Sci. and Eng., Division of Physical Sci., Kanazawa Univ., Kakuma, Kanazawa 920-11, Japan.*

** *Fac. of Education, Kanazawa Univ., Kakuma, Kanazawa 920-11, Japan.*

with alkali hydroxyl.

We recently reported[13)-17)] on the optical properties of a blue emission at 420 nm in addition to the characteristic 360 nm emission in NaCl:Cu^+ crystals containing OH^- ions. As a result, it has been demonstrated that the origin of the former is presumably attributed to a Cu^+ defect perturbed by a neighboring OH^- defect, while the latter is, as well known, attributed to an isolated Cu^+ defect[18)].

It is the purpose of this paper to ascertain the origin and the optical properties of the 420 nm emission through systematic experiments. Moreover, the origin of its emission is qualitatively discussed and the activation energy corresponding to its transition is also estimated.

Experimental

In our previous paper[15)] to pursue the origin of the blue emission at 420 nm, Cu incorporation was performed by a diffusion technique to incorporate a constant amount of Cu^+ ions into the NaCl crystals containing various OH^- concentrations. In this work to find out the optimum quantities of Cu^+ and OH^- concentrations for the enhancement of the blue emission, additional NaCl cystals were grown by the Kyropoulos method in our laboratory adding appropriate amounts of CuCl and NaOH.

The excitation and emission spectra were taken with a Hitachi F-3010 spectrofluorometer, while the absorption spectra were taken with a Hitachi U-2000 spectrophotometer. For lifetime measurements a universal photon counting system (Hamamatsu Photonics, C2550-01, C2760, R2256P) was used. As the excitation source, a high pressure flash lamp is used, which emits stable light pulses with an fwhm of less than 2 ns and with a repetition rate of 4 kHz. The sample was mounted in a variable temperature cryostat (Oxford, DN-1754) in conjunction with a temperature controller (Oxford, ITC-4). The Cu^+ and OH^- concentrations of each crystal actually used in the measurements were determined by means of the inductively coupled plasma (ICP) method and from the intensity of the ultraviolet

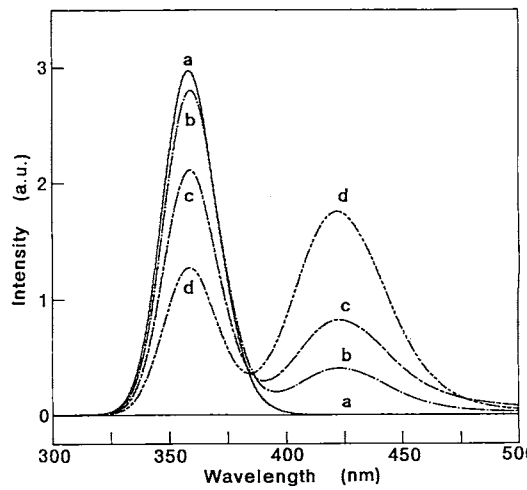

Fig. 1　Emission spectra at RT of NaCl crystals with different Cu^+ and OH^- concentrations; (a) 188 ppm Cu^+, 1.3 ppm OH^-, (b) 143 ppm Cu^+, 57 ppm OH^-, (c) 127 ppm Cu^+, 80 ppm OH^-, and(d) 85 ppm Cu^+, 110 ppm OH^-, respectively.

absorption band due to the electronic transition of OH^- ions at 185 nm[19], respectively.

Results

Firstly, the temperature dependence of a blue emission at 420 nm in an NaCl:Cu^+:OH^- crystal is investigated. Fig. 1 shows the typical emission spectra due to excitation into the 255 nm absorption band at room temperature (RT) of NaCl crystals with different Cu^+ and OH^- concentrations. The Cu^+ and OH^- concentrations for each curve are(a) 188 ppm Cu^+, 1.3ppm OH^-, (b) 143 ppm Cu^+, 57 ppm OH^-, (c) 127 ppm Cu^+, 80 ppm OH^-, and (d) 85 ppm Cu^+, 110 ppm OH^-, respectively. It is seen from the figure that two clear emission bands with maxima at 359.4 and 422.2 nm are observed at RT. We call the former the 360 nm band, while the latter the 420 nm band. Moreover, when the samples contain more Cu^+ ions and less OH^- ions the 360 nm emission band is more exaggerated and the 420 nm band is suppressed.

Fig. 2 shows the emission spectra of an NaCl:Cu^+:OH^- sample (corresponding to that of Fig.1, curve d) produced by the excitation in the 255 nm band at various temperatures in the range from 77 to 288 K (RT). At the temperature between 150 K (curve c) and 200 K (curve d) the wavelength shifts drastically from about 395 to 420 nm can be seen. Therefore, the emission spectra were measured as a function of stepwise increasing temperatures from 158 (curve a) to 199 K (curve f) as shown in Fig. 3 . It should be noted here that the peak position and its intensity of the 360 nm band are almost independent of the measuring temperature, while those of the

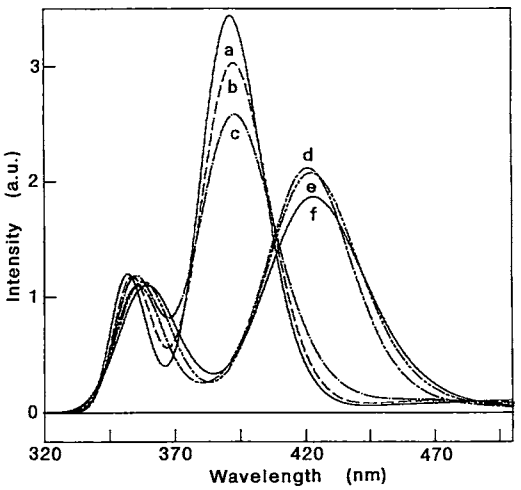

Fig. 2 Emission spectra of an NaCl:Cu^+ (85 ppm): OH^- (110 ppm) sample at various temperatures; (a) 77, (b) 100, (c) 150, (d) 200, (e) 250, and (f) 288 K (RT).

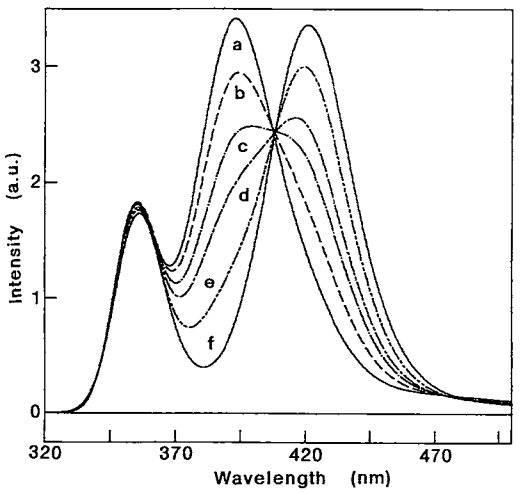

Fig. 3 Stepwise emission spectra of the same sample as in Fig. 2 at various temperatures from 158 to 199 K ; (a) 158, (b) 164, (c) 169, (d) 173, (e) 181, and (f) 199 K.

Table 1　Peak wavelengths of absorption, excitation, and emission bands at RT and 77 K in an $NaCl:Cu^{+}:OH^{-}$ crystal.

Crystal	Temp.	Absorption (nm)	Excitation		Emission	
			360nm Band (nm)	420nm Band (nm)	360nm Band (nm)	420nm Band (nm)
$NaCl:Cu^{+}:OH^{-}$	RT	254.0	257.2	252.8	359.4	422.2
	77K	255.2	257.6	252.0	353.2	394.8

420 nm band are strongly dependent on the temperature. These peak positions shift towards longer wavelength by 6 nm for the former and by 27 nm for the latter as the temperature increases from 77 K to RT. In contrast to this, no shift in peak positions is observed for the excitation spectra of both emission bands in the temperature range from 77 K to RT as shown in Table 1. These results indicate that the two different emissions originate from two different configurations of the relaxed excited state (RES) since not any spectral shift in the optical absorption of the defect-pair is observed around 170 K. Moreover the fact that all the curves in Fig. 3 cross at a constant point imparts an important support to the origin of the two emission peaks, at least, a one-to-one correspondence of the two centers.

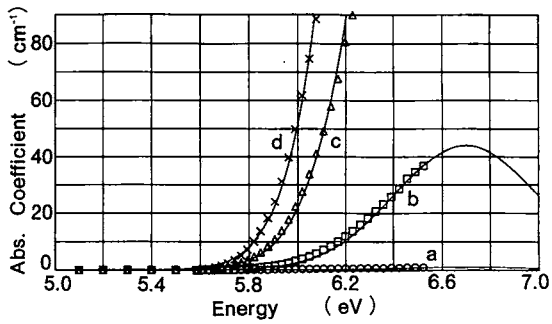

Fig. 4　Determination of the OH^{-} concentration from the ultraviolet absorption band. The solid curves are the Gaussian tails, the parameters of which were given by Klein et al[19]. The OH^{-} concentrations are estimated to be (a) 1.3, (b) 57, (c) 480, and (d) 1100 ppm.

By the way, at temperatures higher than RT, parallel to the longer wavelength shifts, the peak height of the 420 nm emission band decreases rapidly. If the temperature has been raised above 500 K the 420 nm band disappears temporarily and only the 360 nm band remains. However, after such a thermal treatment, the peak height of the 420 nm emission band recovers slowly ($\sim$ 2 months) up to the initial level when the sample is kept at RT. The data indicate that at temperatures higher than RT the dissociation of the $Cu^{+}:OH^{-} \rightarrow Cu^{+}+OH^{-}$ takes place, and the weakly-coupled OH^{-} ion with the Cu^{+} ion exists as a free ion within the crystal. A similar behavior as described above has been also observed in the formation or decomposition of the $(F_2^{+})_H$ centers[10)11)], i.e., F_2^{+} centers close to the stabilizing impurity [also called $F_2^{+}:O^{2-}$ centers] in NaCl.

Secondly, systematic experiments are performed to clarify the origin of a blue emission. Fig. 4 shows the absorption spectra at RT of NaCl with different OH^{-} concentrations

before Cu incorporation. The concentrations of OH^- ions were determined from the intensity of the ultaviolet absorption band due to the electronic transition of OH^- ions. Since the band peak at 6.7 eV (185 nm) was not measured directly, it was estimated from the tail of the absorption spectra on the low energy side. The observed absorption tails, fit well to the Gaussian curves (solid lines), the parameters of which were determined by Klein et al[19]. We used the conversion rate of 1.3 ppm/cm^{-1} from peak height to OH^- concentration. As a result, the OH^- concentrations were estimated to be 1.3, 57, 480 and 1100 ppm, respectively. In addtion the absence of another impurity, particularly divalent ions in the crystal, which forms complexes[3] with the OH^- ions was ascertained.

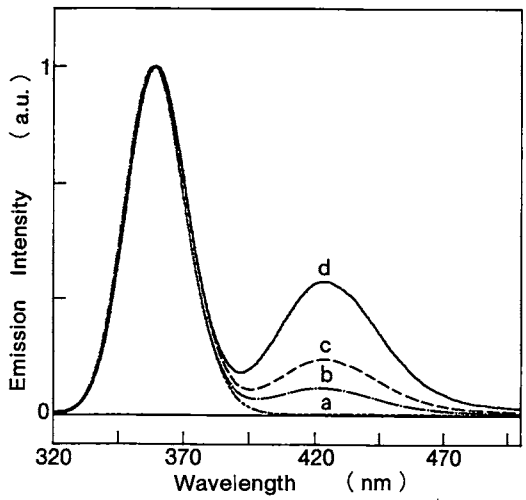

Fig. 5 Emission spectra at RT of NaCl:Cu^+ samples with different OH^- concentrations; (a) 1.3, (b) 57, (c) 480, and (d) 1100 ppm.

Fig. 5 shows the emission spectra of NaCl:Cu^+ samples with different OH^- concentrations. (All curves in Fig. 5 are corresponding to those in Fig. 4 , respectively.) Though Cu incorporation was performed under the same conditions, each sample used here was found to contain different Cu^+ concentrations. The Cu^+ concentrations were determined to be 188, 143, 230 and 441 ppm, respectively, by the ICP method. The postulated constant emission band at 420 nm appears to grow with OH^- concentration and no 420 nm emission band can be entirely seen in the NaCl:Cu^+ sample containing negligible amounts of Cu^+ ions, even if large amounts of OH^- ions are contained in the sample. Moreover, it was also ascertained that the 420 nm emission band does not appear in the sample without containing Cu^+ ions, even if large amounts of OH^- ions are contained. These results indicate that the presence of OH^- and Cu^+ ions is essential to the 420 nm emission band.

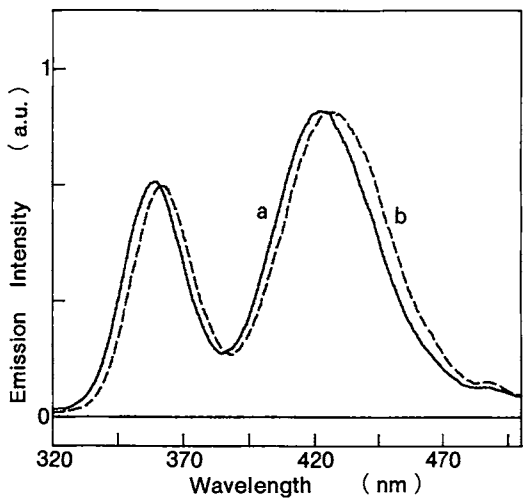

Fig. 6 Emission spectra at RT of as-grown NaCl:Cu^+ samples containing large amounts of (a) OH^- and (b) OD^- ions.

In order to ascertain the postulation described above, we performed isotopic

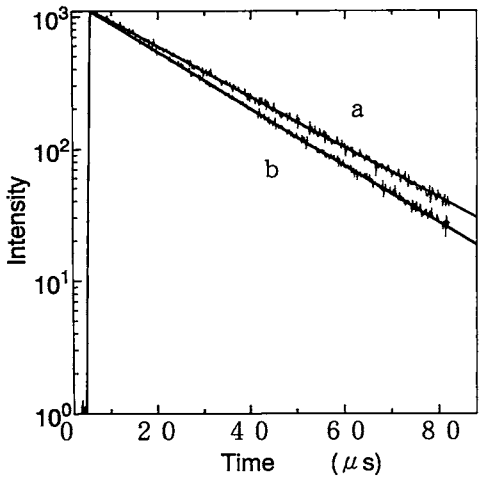

Fig. 7　Typical decay curves of an NaCl:Cu^+:OH^- sample at RT for the (a) 360 and (b) 420 nm emission band.

Table 2　Lifetime values for the (a) 360 and (b) 420 nm emissions at RT and 77 K in an NaCl:Cu^+:OH^- crystal.

Band	Temp. (K)	Lifetime (μs)
360 nm	RT	38.8 38[20]
	77K	81.2 82[20]
420 nm	RT	25.0
	77K	33.3

substitution of OD^- for OH^- in NaCl:Cu^+. Fig.6, curves a and b show the emission spectra at RT of as-grown NaCl:Cu^+ samples containing large amounts of OH^- ions and OD^- ions, respectively. In the case of OD^--doped NaCl:Cu^+, each peak position shifts towards longer wavelength by 2 nm for the 360 nm band and by 6 nm for the 420 nm band. This result supports that the 420 nm emission band may be ascribed to complexes or associates containing Cu^+ and OH^- ions.

Fig. 7 curves a and b show typical luminescence decay curves of the 360 and 420 nm emissions at RT, respectively. The dots are data points. The straight line is the best fit to the decay curve. These curves are purely single exponential over nearly three orders of magnitude in time. The lifetime values for the 360 nm and 420 nm emissions at RT and 77 K are summarized in Table 2. It should be noted that the lifetime values obtained here, 38.8 μs at RT and 81.2 μs at 77 K, for the 360 nm emission agree well with those, 38 μs at RT and 82 μs at 77 K, reported by Bertolaccini et al.[20]

Discussion

In order to analyze such a thermal equilibrium shown in Figs. 2 and 3, the following formula was applied, which was introduced by Aegerter and Luty[21] for investigating a thermally activated Arrhenius process over an energy barrier ΔE from the primary RES into a new RES configuration with different emission for the F_2^+ center in KCl.

The observed temperature dependence of the relative quantum efficiency, η_{395}, for the 395 nm band can be described by the relation

$$\eta_{395} = \frac{1}{1 + \nu\,\tau \exp\,(-\Delta E/kT)}, \qquad (1)$$

where k is the Boltzmann constant. $\nu\ \tau$ is the product of RES lifetime τ and Arrhenius attempt frequency ν. This relation describes the thermal quenching of an emission process by a temperature activated radiationless process. The quantum efficiency of the 420 nm band, η_{420}, is given by $\eta_{420}=1-\eta_{395}$. It is clear from eq. (1) that on a semilogarithmic scale $1/\eta - 1$ as a function of the reciprocal temperature, $1/T$, the slope of the curve corresponds to the value of $\Delta E/k$. As a result the energy value ΔE and the $\nu\ \tau$ value can be estimated to be $\Delta E=0.20$ eV and $\nu\,\tau = 9.8\times10^5$, respectively. The estimated $\nu\ \tau$ value agrees well with the previously reported one, $\nu\,\tau = 1.2\times10^5$, for the F_2^+ center in KCl[21]. The calculated and measured quantum efficiencies η of the 395 and 420 nm emission are plotted as a function of temperature in Fig. 8. Curves a, b and c show the calculated ones with the parameters of $\Delta E=0.20$ eV and $\nu\,\tau = 1.0\times10^7$, 1.0×10^6 and 1.0×10^5 for the 395 nm emission, respectively. Curve d shows the same one with the parameters of $\Delta E=0.20$ eV and $\nu\,\tau = 1.0\times10^6$ for the 420 nm emission. The measured relative efficiencies η as a function of temperature for the 395 (○) and 420 nm (△) emissions are also plotted by reconstructing the emission spectra in Figs. 2 and 3. Moreover, with the lifetime values shown in Table 2 for the 420 nm emission at RT and 77 K the attempt frequency for the competing radiationless process is obtained from the measured $\nu\,\tau = 9.8\times10^5$ to be $\nu_{395}=2.9\times10^{10}\ s^{-1}$ and $\nu_{420}=3.9\times10^{10}\ s^{-1}$, respectively.

Though there may be many considerations for the explanation of the above experimental fact, we may propose a model. According to the results given by Suto et al.[22] the OH^- ion in NaCl is substituted for a chlorine ion and is located at the ⟨100⟩ off-center positions by 0.085 nm. In addition, according to the data of Paus and Luty[23], the OH^- ion rotates freely at RT and the OH^- ion diameter is 0.272 nm and is significantly smaller than the diameter of a chlorine ion (0.334 nm) it places. On the contrary, no expansion or contraction takes place when the Cu^+ ion replaces the Na^+ ion in NaCl because these ions have about the same radius. Therefore, the Cu^+ ion in NaCl occupies an on-center position[24,25]. However, it may be proposed that the substitutional Cu^+ ions in

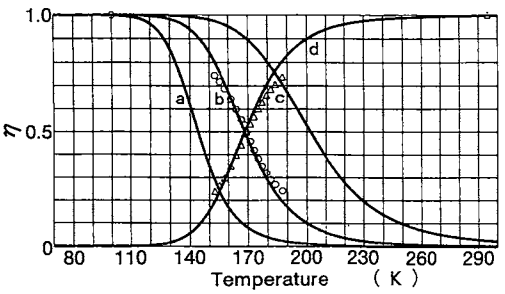

Fig. 8 Calculated and measured quantum efficiencies η of the 395 and 420 nm emissions as a function of temperature. Curves a, b, and c show the calculated ones with the parameters of $\Delta E=0.20$ eV and $\nu\,\tau = 1.0\times10^7$, 1.0×10^6 and 1.0×10^5 for the 395 nm emission, respectively. Curve d shows the same one with the parameters of $\Delta E=0.20$ eV and $\nu\,\tau = 1.0\times10^6$ for the 420 nm emission. (○) and (△) show the measured quantum efficiencies as a function of temperature for the 395 and 420 nm emissions, respectively.

NaCl are affected by the presence and the movement of the OH^- ion and thus the drastic behavior of the 420 nm band which appeared at the temperature of ~170 K is considered to be due to a shortrange rearrangement of the Cu^+:OH^- center causing a transition between Cu^+ positions of high or low perturbation of the OH^- ions. This result yields further for the origin of the blue emission at 420 nm in addition to the isotopic substitution data (Fig. 6) and the in combination with luminescence lifetime measurements (Fig. 7 and Table 2).

In conclusion, the systematic measurements to clarify the origin and the optical properties of the 420 nm emission in an NaCl:Cu^+:OH^- crystal have been performed. As a result, it is acertained that the blue emission at 420 nm originates from a Cu^+ defect perturbed by a nearest neighboring OH^- defect and its drastic behavior at the temperature of ~170 K corresponds to a short-range rearrangement of the Cu^+:OH^- defects. It has been also demonstrated that the quenching of the 395 nm emission and the enhancement of the 420 nm emission can both be described by a thermally activated process characterized by $\Delta E=0.20$ eV and $\nu\ \tau=9.8\times10^5$. Moreover the enhancement of the blue emission band at 420 nm in comparison with the 360 nm band has been realized by adding the appropriate amounts of Cu^+ and OH^- concentrations.

References

1) T.G.Stoebe, J. Phys. Chem. Solids **28**, 1375 (1967).
2) W.Känzig, H.R.Hart, Jr., and S.Roberts, Phys. Rev. Lett. **13**, 543 (1964).
3) H.W.Etzel and D.A.Patterson, Phys. Rev. **112**, 1112 (1958).
4) F.Kerhoff, W.Martienssen, and W.Sander, Z. Phys. **173**, 184 (1963).
5) L.F.Mollenauer, in: *Tunable Lasers*, Eds. L.F.Mollenauer and J.C.White, Springer-Verlag, Berlin 1987 (Chap. 6).
6) W.Gellermann, J. Phys. Chem. Solids **52**, 249 (1991).
7) L.F.Mollenauer, Opt. Lett. **6**, 342 (1981).
8) J.F.Pinto, L.Stratton, and C.R.Pollock, Opt. Lett. **10**, 384 (1985).
9) D.Wandt, W.Gellermann, F.Luty, and H.Welling, J. Appl. Phys. **61**, 864 (1987).
10) E.Georgiou, J.F.Pinto, and C.R.Pollock, Phys. Rev. **B 35**, 7636 (1987).
11) G.Lifante, P.Silfsten, and F.Cusso, Phys. Rev. **B 40**, 9925 (1989).
12) D.Wandt and W.Gellermann, Opt. Commun. **61**, 405 (1987).
13) T.Kurobori, S.Taniguchi, and N.Takeuchi, J. Mater. Sci. Lett. **11**, 1140 (1992)
14) T.Kurobori, S.Taniguchi, and N.Takeuchi, phys. stat. sol. (b) **172**, K 77 (1992).
15) T.Kurobori, S.Taniguchi, and N.Takeuchi, J. Lum. **55**, 183 (1993).
16) T.Kurobori, H.Yonezawa, and N.Takeuchi, J. Lum. **59**, 157 (1994).
17) T.Kurobori and N.Takeuchi, phys. stat. sol. (to be published).
18) M.Herreros and F.Jaque, J. Lum. **9**, 380 (1974).
19) M.V.Klein, S.O.Kennedy, T.I.Gie, and B.Wedding, Mater. Res. Bull. **3**, 677 (1968).
20) M.Bertolaccini, P.Gagliardelli, G.Padovini, and G.Spinolo, J. Lum. **14**, 281 (1976).
21) M.A.Aegerter and F.Luty, phys. stat. sol. (b) **43**, 245 (1971).
22) S.Suto and M.Ikezawa, J. Phys. Soc. Japan **53**, 438 (1984).

23) H.Paus and F.Luty, phys. stat. sol. **12**, 342 (1965).
24) W.D.Wilson, R.D.Hatcher, R.Smoluchowski, and G.J.Dienes, Phys. Rev. **184**, 844 (1969).
25) M.Piccirilli and G.Spinolo, Phys. Rev. **B 4**, 1339 (1971).